OPTICAL SPECTROSCOPY OF MICROCAVITIES

A.SERPENGÜZEL
Physics Department, Bilkent University, Ankara, 06533 Turkey
S.ARNOLD
Physics Department, Polytechnic University, Brooklyn, New York 11201 USA
G.GRIFFEL
Department of Electrical Engineering, Polytechnic University, Brooklyn, New York 11201 USA
AND
J.A.LOCK
Physics Department, Cleveland State University, Cleveland, Ohio 44115 USA

Abstract.
Microcavities, such as microspheres, possess morphology-dependent resonances (MDR's). In this chapter light coupling mechanisms to MDR's is examined. The novel mechanism of excitation of the microsphere with an optical fiber coupler (OFC) provides spatially and spectrally selective, as well as enhanced light coupling to the MDR's, when compared with the conventional plane wave excitation. The plane wave excitation is described by Lorenz-Mie Theory. However, Generalized Lorenz-Mie Theory and the Localization Principle are used for the OFC excitation.

1. Introduction

In recent years, the quantum confinement and localization effects in small scale systems have attracted substantial attention. Physical properties of these systems make them promising for applications in nonlinear optics and optoelectronic device physics. Available examples are micrometer-size droplets, polystyrene microspheres, doped and undoped optical fibers, colloids, glasses doped with semiconductor microcrystallites, and quantum well, wire, dot, and superlattice structures. These structures have well characterized electromagnetic properties, and due to their morphology they act as optical cavities at specific frequencies, thereby resulting in the localization of light, and affecting the dispersive properties of the medium.

Microspheres, specially, continue to enjoy the attention of the optical spectroscopy community, because of their unique optical properties. [1] In the terminology of Photonic Band Gaps (PBG's), [2, 3] these microspheres are the equivalent of "Photonic Atoms", [4] since they can be used as a building block for the "Photonic Crystals". [5]

T. Hakioğlu and A. S. Shumovsky (eds.), Quantum Optics and the Spectroscopy of Solids, 237–248.

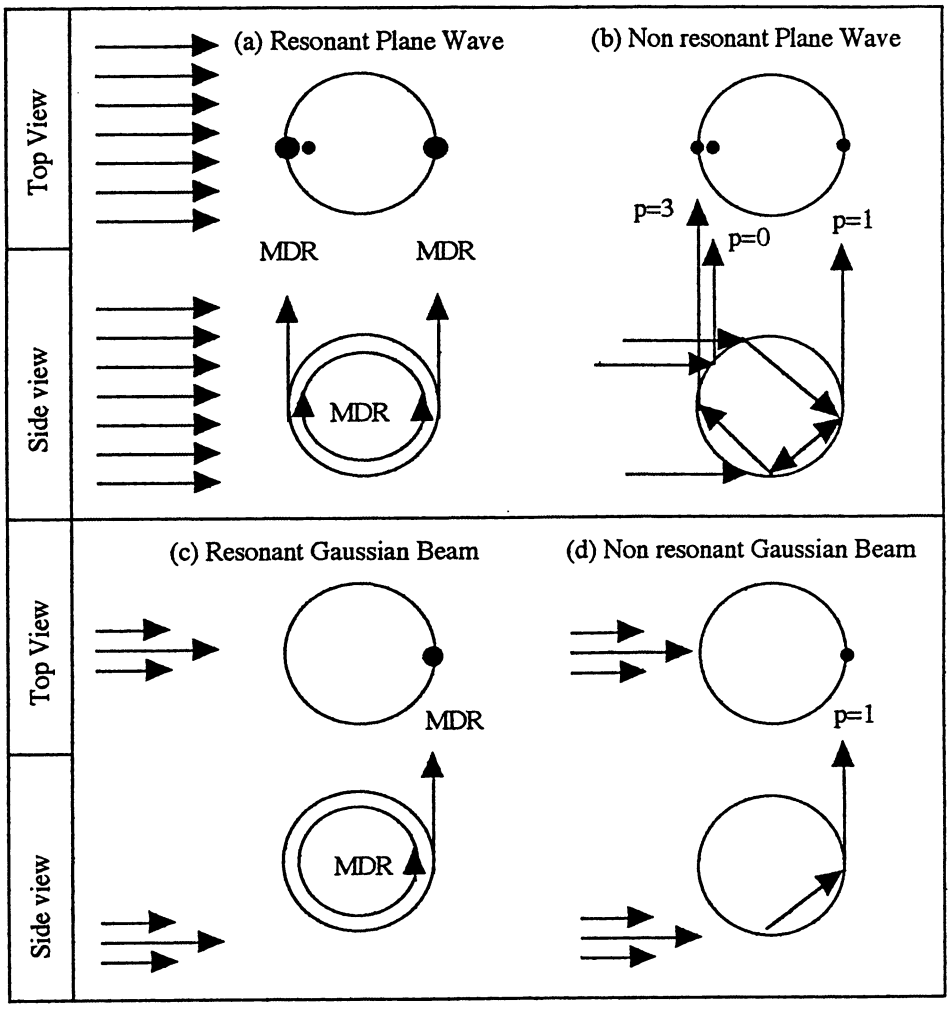

Figure 1. Schematic of the top and side views of the microsphere depicting the non- resonant (p=0,1,3) glare spots and MDR glare spots when excited by (a) a resonant plane wave, (b) a non-resonant plane wave, (c) a resonant off-axis Gaussian Beam, and (d) a non-resonant off-axis Gaussian Beam. Note that the glare spots are not totally correlated with the internal intensity distributions.

The curved interface of the microsphere is responsible for three electromagnetic and quantum-electrodynamic (QED) effects. First, for a plane wave illumination, the internal intensity is concentrated along the principal diameter near the front and the back surfaces of the microsphere (Fig. 1(b) and Fig. 2).

For a droplet with radius a = 35μm, and refractive index N=1.36, an intensity enhance-

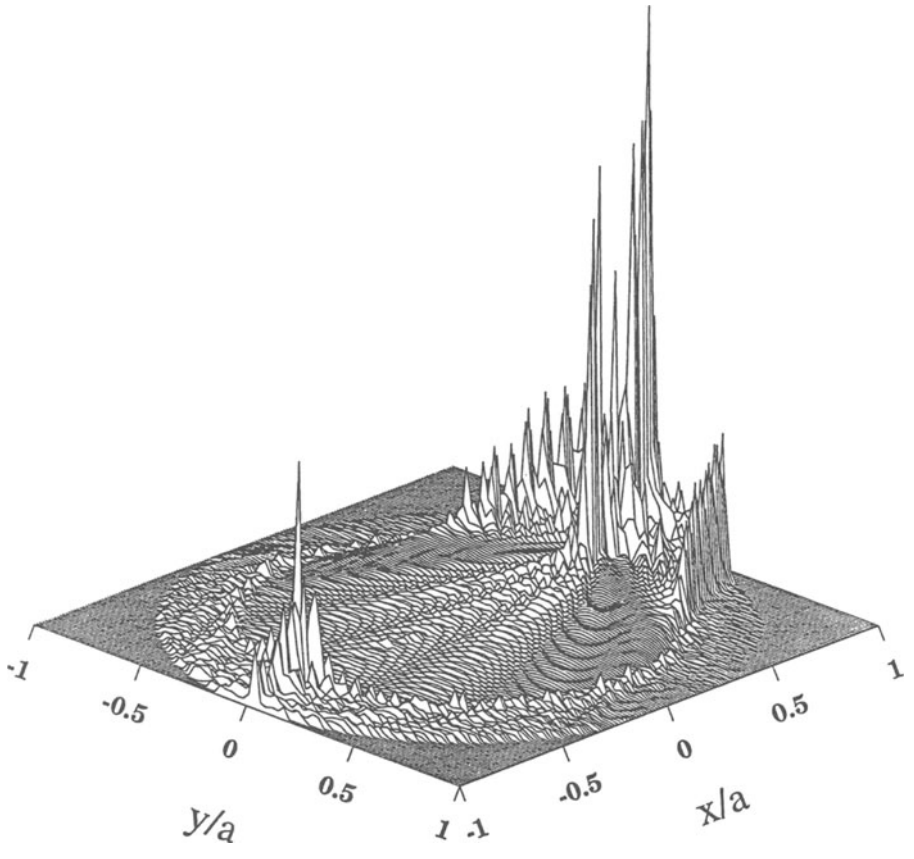

Figure 2. The internal input-laser intensity distribution in the equatorial plane of the droplet for a plane-wave input (off resonance) propagating in the x-direction with size parameter x =418 and N=1.36.

ment of approximately 100X (and 10X) is expected in the localized region just within the droplet shadow (and illuminated) face. These intensity enhancement factors increase with the droplet radius, because more of the incident radiation is intercepted by the droplet illuminated face or hemisphere. Second, the microsphere acts as an optical cavity for specific wavelengths, which satisfy the morphology-dependent resonance (MDR) condition. MDR's can be considered as standing waves, which may be decomposed into two coun-

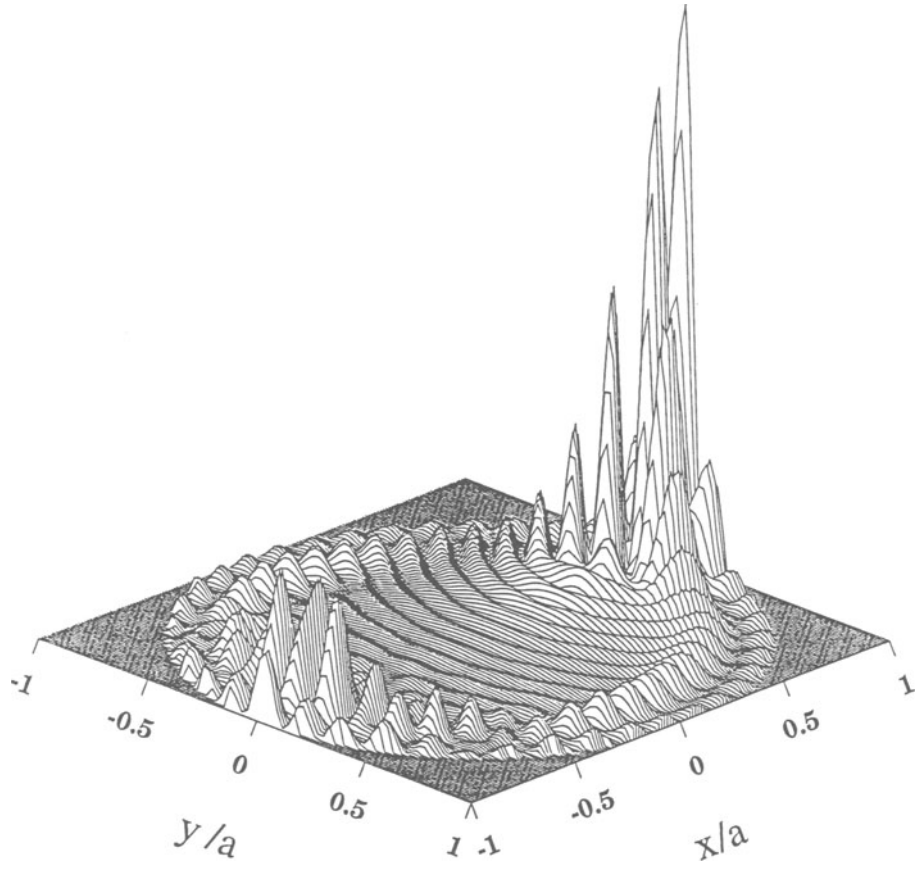

Figure 3. The internal intensity distribution in the equatorial plane of the droplet for a plane-wave input [on an input (TE) resonance] propagating in the x-direction with N=1.59, x=18.83. The maximum value of the internal intensity is 159.

terpropagating waves traveling around the microsphere rim (Fig. 1(a) and Figs. 3-4). The counterpropagating traveling waves must experience quasi-total-internal reflection repeatedly at the spherical droplet interface and return to the starting point with their initial phase. For wavelengths that are on MDR's and within the medium's gain profile, the generated output waves circulate around the droplet rim and experience gain at the two high internal intensity regions. Occasionally, when the monochromatic input-laser frequency is

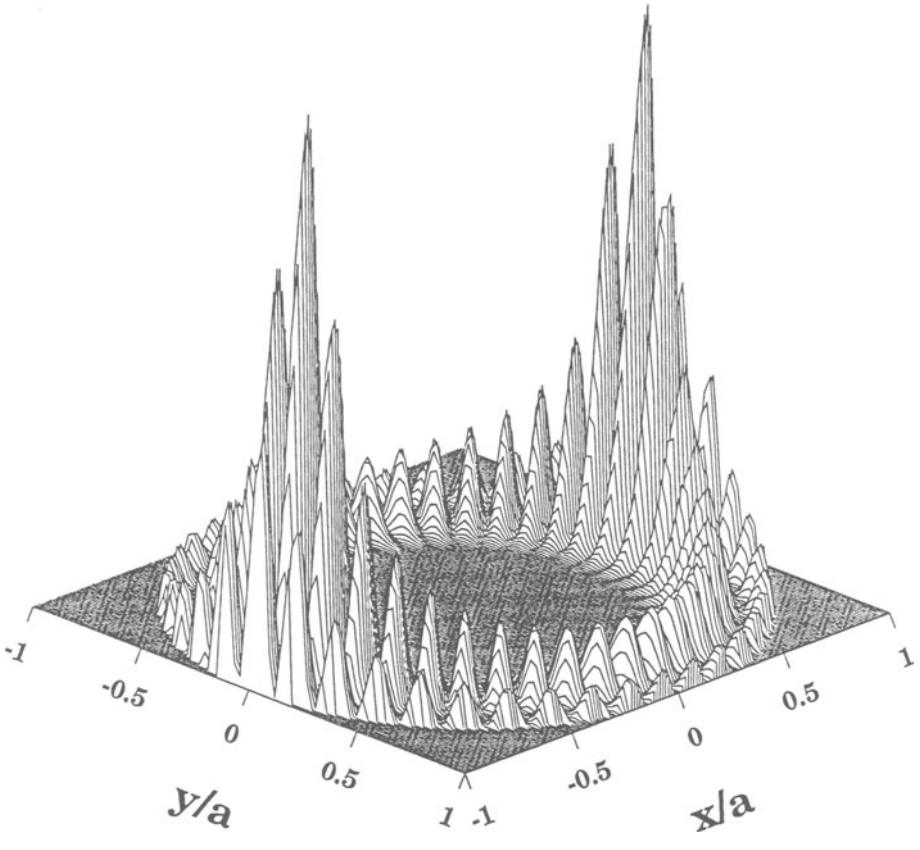

Figure 4. The internal intensity distribution in the equatorial plane of the droplet for a MDR [an output (TE) resonance] with N=1.59 and x =18.83. Notice that the internal intensity due to the focusing of the plane wave input of the Fig. 3 is missing, and the maximum value of the internal intensity is 49 as opposed to 159 of Fig. 3.

tuned to a MDR (an input resonance), there can be an even larger enhancement the input intensity (Fig. 4). Third, the optical transition cross-sections in the microspheres can be larger than bulk optical transition cross-sections, because of the modified density of final electromagnetic states. [6] In the microsphere, the final electromagnetic states correspond to the microsphere cavity resonances, which are described by MDR's. For a bulk sample,

however, the final electromagnetic states are the continuum modes of an infinite system. [7, 8]

The SRS threshold for a water microdroplet is lower than that of water in an 11-cm optical cell.[9] In addition, these three effects are responsible for the occurrence of a number of other nonlinear optical effects such as stimulated anti-Stokes Raman scattering (SARS),[10] coherent anti-Stokes Raman scattering (CARS),[11] stimulated Brillouin scattering (SBS),[12] third-harmonic generation (THG),[13, 14] and lasing [15, 16, 17] in microdroplets.

If the incident plane wave is resonant with a MDR (i.e., on-resonance), there will, in addition, be a uniform intensity distribution within the rim of the microsphere in the volume determined by the MDR (Fig. 1(a)). [18] However, if an off-axis Gaussian beam is used at a resonant wavelength, the internal intensity is only distributed within the rim of the microsphere in the volume determined by the MDR, and is no longer concentrated near the front and the back surfaces of the microsphere (Fig. 1(c)). [19] Therefore, a resonant off-axis Gaussian beam excites the MDR's more uniformly and more efficiently than a plane wave. Even edge illumination with a focused beam excites MDR's more efficiently than plane waves (Fig. 1(d)). [20, 21] The off-axis Gaussian beam calculations have recently been realized using generalized Lorenz-Mie theory (GLMT). [22, 23]

2. Experiments

The first experimental realization of the off-axis Gaussian beam excitation geometry was performed by using an optical fiber coupler (OFC). [24] The frequency shift and linewidth broadening of the MDR's due to the OFC-microsphere interaction were also studied. [25] In these OFC- microsphere experiments the cladding of the fiber was not index matched to the media surrounding the microsphere, so that there was an optical interface at the OFC surface. In this chapter, we describe the excitation of the MDR's of a microsphere resting on the surface of an OFC, whose surface has been wetted with an index matching oil to eliminate the air- fiber interface. Thereby, the beam in the optical fiber effectively becomes the equivalent of a Gaussian Beam with an infinitely long skirt length.

Figure 5 is a schematic of our experimental setup. A polystyrene (PS) microsphere with an approximate radius a = 12 μm and refractive index N = 1.59 is placed on an OFC. The OFC is made from a single-mode optical fiber (SMOF) with a core diameter of 3.8 μm (N = 1.462), and a cladding diameter of 125 μm (N = 1.457). The cladding below the microsphere is shaved down to 0.7 μm. The SMOF mode has approximately a Gaussian intensity profile and is doubly degenerate with both horizontal and vertical polarizations. The OFC surface and the microsphere were wetted by a few millimeters of index matching oil (N = 1.456, same as the cladding). The excitation is provided by a tunable and linearly polarized CW dye laser with a linewidth of 0.025 nm. The dye laser is coupled to the SMOF with a microscope objective. Although the output of the dye laser was linearly polarized, the output from the SMOF was observed to be elliptically polarized due to the fiber birefringence. Therefore, the OFC provides both linear polarizations to the microsphere. The scattering from the microsphere was collected at 90° with a microscope objective followed by a polarizer, and detected with a photomultiplier tube.

If plane wave illumination were used, the image of the microsphere (either on resonance or off resonance) would show three principal glare spots (Fig. 1(a-b)). [26] However, in our

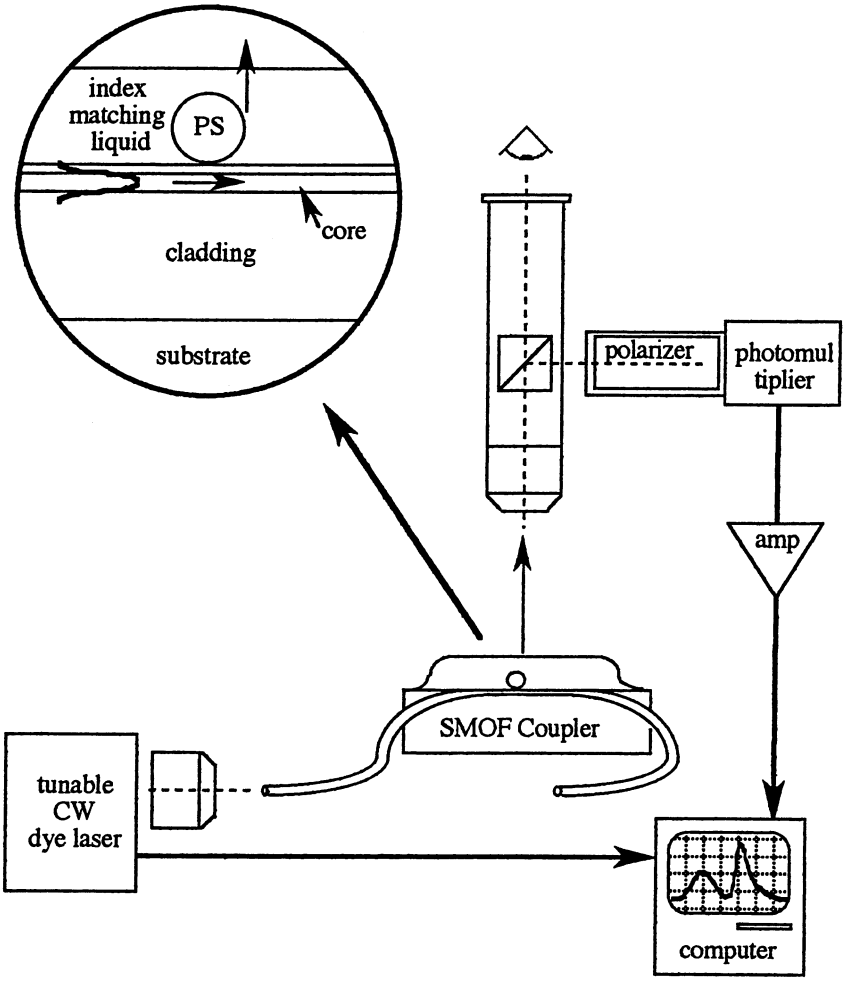

Figure 5. Schematic of the experimental setup with inset to depict the microsphere on the wetted surface of the SMOF coupler.

case of coupling an external beam from the SMOF, we observe only one glare spot on the far side of the microsphere (Fig. 1(c)). In contrast to the non-index matched case, this far side glare spot is observed for all laser wavelengths, even when the incident wavelength is not on a MDR (i.e., off-resonance). However, when the incident light is on-resonance, the far side glare spot intensity is enhanced by a factor of about 2. Apparently, the standing wave pattern which was set up by a plane wave excitation of a MDR, with its counterpropagating traveling waves (Fig. 1(a)), is replaced with a single counter-clockwise traveling wave in

the Gaussian beam excitation (Fig. 1(c)). Also, in the Gaussian beam excitation (Fig. 1(c-d)), the off-resonance glare spots are due to refraction only (i.e., p=1 rays), while for a plane wave illumination the off-resonance glare spots are due to both refraction (i.e., p=1,3 rays) and specular reflection (i.e., p=0 rays).

3. Theory of off-axis Gaussian beam excitation

Figure 6(a) displays the experimentally observed transverse electric (TE) scattering spectrum from the microsphere excited with the OFC. Figure 6(b) depicts the theoretically calculated TE scattering spectrum for an off-axis Gaussian beam placed at the location of the OFC. Comparing the spectra in Fig. 6 to the scattering spectra obtained with a plane wave, one notices two features: (1) there is a large background intensity, which cannot be explained by the light scattered due to OFC surface imperfections; and (2) the MDR's have nearly Lorentzian lineshapes as opposed to the Fano lineshapes [27] of the plane wave scattering spectra. Most of the prominent features of these scattering spectra are described by the interaction of the microsphere with an external beam having a Gaussian intensity profile and propagating at an impact parameter (b), which is slightly greater than the microsphere radius (a). Since the excitation by such a beam occurs beyond the edge of the microsphere, the light scattering can be calculated by (i) removing the partial waves with angular momentum quantum numbers (n) less than the size parameter (x, which is the ratio of the perimeter of the microsphere to the incident light wavelength) from the conventional Lorenz-Mie (plane wave excitation) infinite series, and (ii) applying generalized Lorenz-Mie theory (GLMT) to parametrize the incident beam profile. This removal of partial waves is justified by the localization principle, [28] which associates a light ray having an impact parameter (b) with a partial wave with mode number (n).

Plane wave Lorenz-Mie theory restricts the angular momentum quantum number (n) range of the light rays, passing by the microsphere surface but yet interacting with it, to have their mode number (n) between x and Nx, where N is the relative refractive index of the microsphere with respect to the outside medium. This condition, together with the localization principle, restricts the impact parameter (b) range to be between a and Na. Therefore, only the light rays within this impact parameter range can couple to the MDR's of the microsphere.

To check the validity of this approach and to simulate our experimental results of Fig. 6(a), we have used the GLMT computation algorithm, [29] which can be applied to on- and off-axis focused Gaussian beam excitation geometries. In GLMT, the plane wave expansion coefficients (a_n for TM or b_n for TE resonances) are replaced by the partial wave expansion coefficients (a_{nm} for TM coefficients or b_{nm} for TE coefficients). For example for TE contributions, $b_{nm} = b_n\ B_{nm}$, where B_{nm} describes the angular overlap of the excitation field and the spherical harmonics.

For our external off-axis Gaussian beam excitation geometry, B_{nm} become significant as n exceeds x. As n is increased further, B_{nm} goes through a series of resonances (i.e., MDR's), with none seen beyond n=Nx. The background in the spectra of Fig. 6(b) is due to the refraction for non-resonant partial waves with n$\downarrow$x. For a plane wave excitation, B_{nm} would have been significant for all n. For the calculations of Fig. 6(b), we used a Gaussian beam (with an infinite skirt-length and a beamwaist with a half-width w_o = 2.176 μm) propagating at an impact parameter of 14.94 μm from a microsphere (with a = 12.34 μm and a relative refractive index of 1.09). The calculation of the scattered

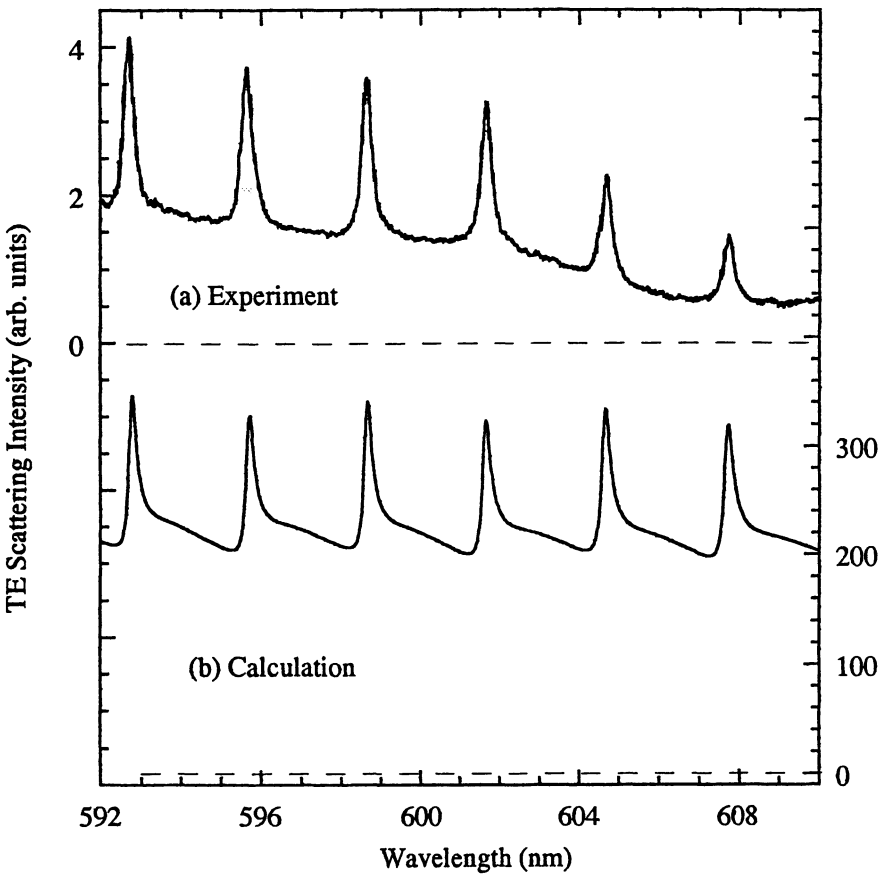

Figure 6. Scattering intensity of (a) experimental, and (b) calculated TE polarized spectrum for a PS microsphere in index matching liquid (N=1.456).

intensity is averaged over the scattering angle around 90°. The results of this calculation are compelling. The theoretical MDR's for an off-axis incidence bear a good relationship to the experimental data [Figs. 6(a)], and appear to correspond to first order MDR's with theoretical quality factors (Q's) of approximately 2000. The mode numbers (n) for the MDR's are within the range of n = 194 -198.

By using the localization principle, we can estimate, where the beam should have been

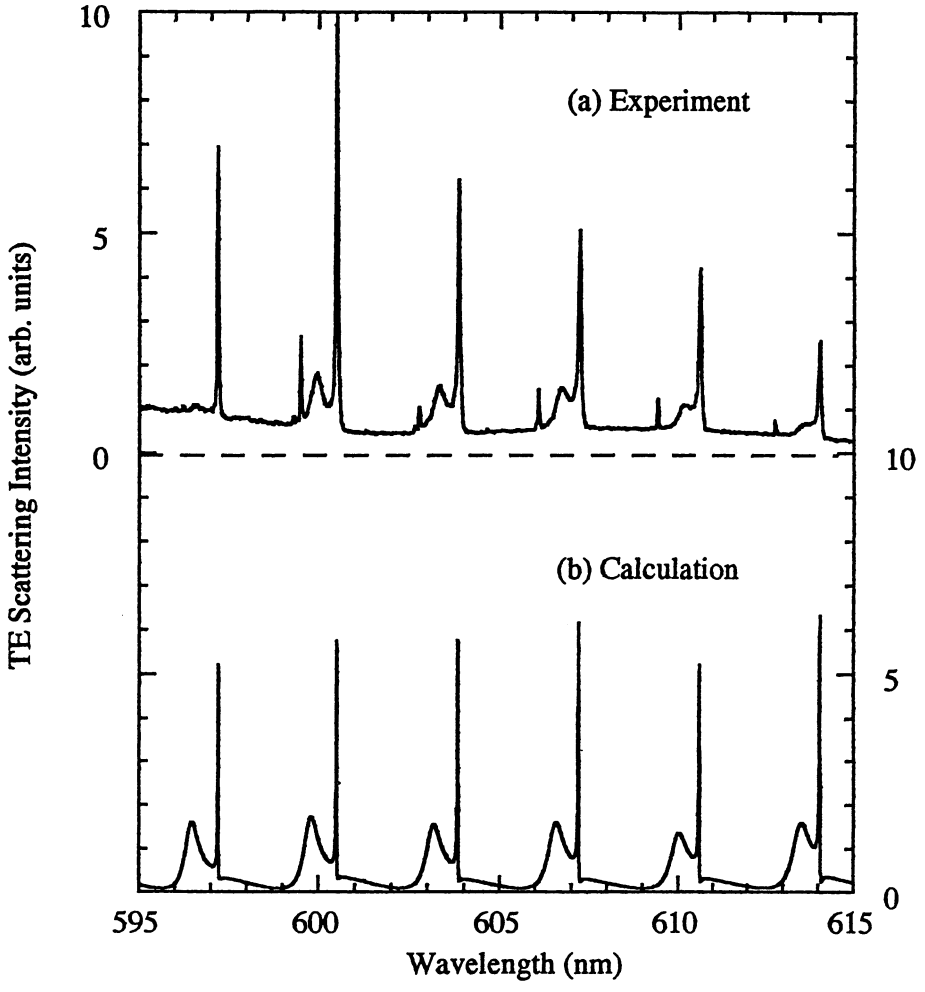

Figure 7. Scattering intensity of (a) experimental, and (b) calculated TE polarized spectrum for a PS microsphere in water (N=1.18).

placed to maximally excite these MDR's with n = 194 -198. We obtain b = n/k = 12.9 μm, which is smaller than our experimental value of b = 14.94 μm. Therefore, we are not coupling to these MDR's with n = 194 -198 with maximal efficiency. Different mode numbers are excited at different impact parameters. For our modes with n = 194-198, in accordance with the localization principle, the maximum of the scattering efficiency occurs at an impact parameter of 12.9 μm. At our impact parameter of 14.94 μm, the

scattering efficiency is less than 0.01. In order to couple most efficiently to our modes with n = 194-198, we would have had to excite the microsphere at an impact parameter of 12.9 μm.

However, efficient coupling is not sufficient for maximum energy storage in the microsphere. The total energy that can be stored in the mode is proportional to the lifetime of that mode, which can further be enhanced with the use of a higher refractive index contrast between the PS microsphere and its surrounding medium, e.g., when N = 1.09 (index matching liquid) is replaced by N = 1.18 (water). Although the water results are more difficult to simulate due to the refractive index step at the cladding-water interface, and the excitation electric field being evanescent rather than being Gaussian, it is possible to have modes with higher measured Q's of 24000. Figure 7(a) shows the experimental elastic scattering intensity of the TE polarized spectrum for a PS microsphere in water (N = 1.18), while Figure 7(b) displays the corresponding calculated spectrum. A noteworthy feature of the spectra in Fig. 7(a) is that, MDR's with linewidths as narrow as 0.04 nm were observed. Since our dye laser has a linewidth of 0.025 nm, the measured MDR linewidths are clearly limited by the convolution of our dye laser linewidth.

4. Conclusion

In conclusion, the microsphere-optical fiber system with the index matching geometry has proved to be very useful in the verification of the generalized Lorenz-Mie theory (GLMT) and the localization principle. The microsphere-optical fiber system also shows promise as a possible building block for photonic memories, [30] and can be used as an external cavity feedback system to line narrow a broader light source such as a diode laser. [31, 32]

Acknowledgements

We are grateful for the partial support of this research from the United States Air Force Office of Scientific Research (Grant Number F49620-94- 0195).

References

1. P. W. Barber and R. K. Chang, Eds., *Optical Effects Associated with Small Particles* (World Scientific 1988) Singapore.
2. E. Yablonovitch, Phys. Rev. Lett. **58**, 2059 (1987).
3. C. M. Soukoulis, *Photonic Band Gaps and Localization* (Plenum Press 1993) New York.
4. S. Arnold, J. Comunale, W.B. Whitten, J.M. Ramsey, and K.A. Fuller, J. Opt. Soc. Am. B **9** 819 (1992).
5. W. Hu, H. Li, B. Cheng, J. Yang, Z. Li, and D. Zhang, Opt. Lett. **20** 964 (1995).
6. E. M. Purcell, Phys. Rev. **69** 681 (1946).
7. S. C. Ching, H. M. Lai, and K. Young, J. Opt. Soc. Am. B **4** 1995 (1987).
8. S. C. Ching, H. M. Lai, and K. Young, J. Opt. Soc. Am. B **4** 2004 (1987).
9. J.B.Snow, S.-X.Qian, and R.K.Chang, Opt. Lett. **10** 37 (1985).
10. D.H. Leach, R.K.Chang, and W.P. Acker, Opt. Lett. **17** 387 (1992).
11. S.-X.Qian, J.B.Snow, and R.K.Chang, Opt. Lett. **10** 499 (1985).
12. J.-Z. Zhang and R.K.Chang, J. Opt. Soc. Am. B **6** 151 (1989).
13. W.P. Acker, D.H. Leach, and R.K.Chang, Opt. Lett. **14** 402 (1989).
14. D.H. Leach, W.P. Acker, and R.K.Chang, Opt. Lett. **15** 894 (1990).
15. H.-M. Tzeng, K.F. Wall, M.B. Long, and R.K.Chang, Opt. Lett. **9** 499 (1984).
16. S.-X.Qian, J.B.Snow, H.-M. TzEng, and R.K.Chang, Science **231** 486 (1986).
17. H.-B.Lin, A.L.Huston, B.L.Justus, and A.J.Campillo, Opt. Lett. **11** 614 (1986).
18. D.S. Benincasa, P.W. Barber, J.-Z. Zhang, W.-F. Hsieh, and R.K. Chang, Appl. Opt. **26** 1348 (1987).
19. E. E. M. Khaled, S. C. Hill, and P. W. Barber, Appl. Opt. **33** 524 (1994).
20. J. -Z. Zhang, D. H. Leach, and R. K. Chang, Opt. Lett. **13** 270 (1988).
21. J. P. Barton, D. R. Alexander, and S. A. Schaub, J. Appl. Phys. **64** 1632 (1988).
22. J. A. Lock and G. Gouesbet, J. Opt. Soc. Am. A **11** 2503 (1994).
23. G. Gouesbet and J. A. Lock, J. Opt. Soc. Am. A **11** 2516 (1994).
24. A. Serpengüzel, S. Arnold, and G. Griffel, Opt. Lett. **20** 654 (1995).
25. N. Dubreuil, J.C. Knight, D.K. Leventhal, V. Sandoghar, J. Hare, and V. Lefevre, Opt. Lett. 813 **20** (1995).
26. S. Arnold, S. Holler, J. H. Li, A. Serpengüzel, W. F. Auffermann, and S. C. Hill, Opt. Lett. **20** 773 (1995).
27. P. W. Barber and R. K. Chang, Eds., *Optical Effects Associated with Small Particles* (World Scientific 1988) Singapore, p.20.
28. H. C. van de Hulst, *Light Scattering by Small Particles* (Dover, 1981) New York, p. 208.
29. J. A. Lock, Appl. Opt. **34** 559 (1995).
30. S. Arnold, C. T. Liu, W. B. Whitten and J. M. Ramsey, Opt. Lett. **16** 420 (1991).
31. G. Griffel, A. Serpengüzel, and S. Arnold, "Quenching of semiconductor lasers linewidth by detuned loading using spherical cavities morphology dependent resonances," *Proceedings of the IEEE: Frequency Control Conf.*, San Francisco, CA, USA (1995).
32. G. Griffel, S. Arnold, D. Taskent, A. Serpengüzel, J. Connolly, and N. Morris, Opt. Lett. **21** 695 (1996).